Agile and Precision Attitude Maneuver Using Variable Gain Feedback Controller and Modified Steering Law to Reduce CMG Misalignment Disturbance

Takuya KANZAWA, Tatsuya ENDO, Hiroshi KAWAI, and Takanori IWATA

Japan Aerospace Exploration Agency, Tsukuba, Japan

This paper presents feedforward/feedback control laws and a CMG steering law to accomplish high-precision tracking and pointing control during agile maneuvers. Feedforward control input is generated by a polynomial profile to avoid excitations of vibration due to flexible appendages. A variable gain feedback control law using CMG gain is proposed to accommodate the excessive torque command and gimbal rate caused in the vicinity of singularity. Subsequently, the disturbances induced by CMG are discussed and the attitude error due to CMG misalignment is reduced by applying the modified steering law, including the amount of misalignment. The results of numerical simulations show the effectiveness of the control and steering laws.

Keywords: CMG, Maneuver, Precision, Agility, Misalignment

可変ゲインフィードバック制御則と CMG ミスアライメント擾乱低減のための修正駆動則を用いた高速・高精度姿勢マヌーバ

本論文では、CMG を用いた高速姿勢マヌーバを高精度化するための制御則／駆動則を提案する。まず、高速姿勢マヌーバにおいて柔構造振動モードを励起しないようにするため、高次多項式によるトルクプロファイルをフィードフォワード制御により印加する。その際、特異点近傍においてフィードバック制御トルク指令値およびジンバル角速度指令値が過大とならないように、姿勢制御系のゲインを特異点からの距離の指標（CMG ゲイン）に応じて可変とするフィードバック制御を提案する。また、CMG はそれ自体が回転機器固有の擾乱を発生し、それにより制御精度が劣化する。この課題に対処するため、ミスアライメント、摩擦トルク、アンバランスによる擾乱をモデル化し、姿勢制御への影響を評価する。特に、ミスアライメント擾乱による姿勢誤差は、ミスアライメントを含むヤコビ行列を新たに用いて、提案されている CMG 駆動則を修正する汎用的な方法により改善できることを示す。

1. Introduction

Recently, the Control Moment Gyro (CMG) has been employed for the attitude control system (ACS) of some observing missions requiring agile maneuvers, and various CMG steering laws to avoid or escape singularity have been studied.[1-6] While CMG is capable of producing large torque rather than the Reaction Wheel (RW), the accuracy of attitude control by CMG is considered to be one of the significant issues, in addition to the problem of singularity. This paper is concerned with the improvement of tracking and pointing control accuracies during agile maneuvers to realize high-precision observing missions. The feedforward/feedback control laws and steering law are presented to overcome the following three issues: (1) attitude error induced by vibration caused by flexible appendages, (2) excessive gimbal rates in the vicinity of singularity, and (3) attitude error induced by CMG disturbances.

Since almost all spacecraft have flexible appendages such as solar array paddles and antennas, these modes of vibration may be excited by CMG torque input. The vibration will result in degradation; not only in pointing accuracy but also agility, because the spacecraft cannot start observation until the residual vibration has been damped sufficiently. Some input profiles to control the flexible spacecraft without excitation have been proposed,[7,8] and a torque profile based on the feedforward control using CMG is also considered for our approach. In this paper, the torque profile formulated by time polynomial is applied to the spacecraft to suppress the vibration.

To accomplish the precision tracking control, the tracking error for a desired attitude profile should be compensated for by a wide bandwidth feedback controller with high gains. However, if ACS controls the attitude precisely, even when the CMGs are encountering singularity, an excessive feedback torque command will be generated. The gimbal rate command will also become excessive, because the excessive torque required is provided to the steering law. For this reason, the spacecraft will be unable to maintain precise tracking unless a feedback control law which accommodates the torque command near the singularity is implemented. This paper proposes a feedback control law whereby the torque command is adjusted using the variable attitude control gains, which depend on the distance from singularity.

In practice, CMG induces disturbances due to misalignment, gimbal friction, rotor mass imbalances, and so on. These disturbances are transferred to the spacecraft body and degrade its pointing performance.[9,10] To cope with the attitude error due to misalignment disturbance, a method to modify the existing steering law is proposed. In addition, this paper deals with the other two disturbances, because the stick-slip behavior of gimbal friction may cause the limit cycle of spacecraft attitude and the rotor mass imbalances induce undesirable jitter.

The remainder of this paper is organized as follows. First, in Section 2, the equation of motion for spacecraft equipped with 4 CMGs is expressed. Second, in Section 3, the torque profile to suppress the modes of vibration is considered. A variable gain feedback control law is proposed to achieve the precise tracking to the desired attitude profile with the use of an acceptable gimbal rate. Third, in Section 4, the CMG disturbances are modeled, and a steering law to reduce attitude error due to misalignment is proposed. Finally, in Section 5,

numerical simulations are performed to verify the performances of the variable gain feedback control and modified steering laws.

2. Spacecraft Attitude Dynamics

The equations of motion for a spacecraft equipped with a cluster of 4 CMGs are given in the spacecraft body-fixed coordinate $\{\vec{\mathbf{b}}_B\}^T = \{\vec{\mathbf{b}}_{Bx} \;\; \vec{\mathbf{b}}_{By} \;\; \vec{\mathbf{b}}_{Bz}\}$ as follows:

$$\mathbf{I}\dot{\boldsymbol{\omega}} + \tilde{\boldsymbol{\omega}}\mathbf{I}\boldsymbol{\omega} = \mathbf{T}_{CMG} + \mathbf{T}_{DIS} \tag{2.1}$$

where

$$\mathbf{T}_{CMG} = -\left(\dot{\mathbf{H}} + \tilde{\boldsymbol{\omega}}\mathbf{H}\right) \tag{2.2}$$

$$\mathbf{T}_{DIS} = \sum_{i=1}^{4}\left\{\mathbf{C}_{C_i}^{B}(\beta,\delta_i)\cdot\mathbf{T}_{Ci} + \tilde{\mathbf{r}}_{C_iB}\mathbf{C}_{C_i}^{B}(\beta,\delta_i)\cdot\mathbf{F}_{Ci}\right\} \tag{2.3}$$

where $\mathbf{T}_{CMG}$ is an attitude control torque applied by 4 CMGs, $\dot{\mathbf{H}}$ is the total output torque, and $\mathbf{H}$ is the total angular momentum generated by 4 CMGs. When a typical pyramid arrangement with a skew angle of β is considered, as depicted in Fig. 1, $\dot{\mathbf{H}}$ is given by

$$\dot{\mathbf{H}} = h_R\begin{bmatrix} -c\beta c\delta_1 & s\delta_2 & c\beta c\delta_3 & -s\delta_4 \\ -s\delta_1 & -c\beta c\delta_2 & s\delta_3 & c\beta c\delta_4 \\ s\beta c\delta_1 & s\beta c\delta_2 & s\beta c\delta_3 & s\beta c\delta_4 \end{bmatrix}\begin{bmatrix}\dot{\delta}_1\\ \dot{\delta}_2\\ \dot{\delta}_3\\ \dot{\delta}_4\end{bmatrix}$$

$$\equiv h_R\mathbf{A}(\beta,\delta_i)\cdot\dot{\boldsymbol{\delta}} \quad (i=1\sim4) \tag{2.4}$$

$\mathbf{A}$ is Jacobian and h_R is an individual angular momentum. $\mathbf{T}_{DIS}$ is a disturbance torque induced by 4 CMGs. Using Eq. (2.3), the disturbance force $\mathbf{F}_{Ci}$ and torque $\mathbf{T}_{Ci}$ for i-th CMG with respect to the gimbal-fixed coordinate $\{\vec{\mathbf{b}}_{Ci}\}$ are transformed to the total disturbance torque $\mathbf{T}_{DIS}$ with respect to the coordinate $\{\vec{\mathbf{b}}_B\}$. $\mathbf{C}_{C_i}^{B}$ is a direction cosine matrix depending on the skew angle β and i-th gimbal angle δ_i. $\mathbf{r}_{C_iB}$ is a position vector from origin O_B to origin O_{C_i}.

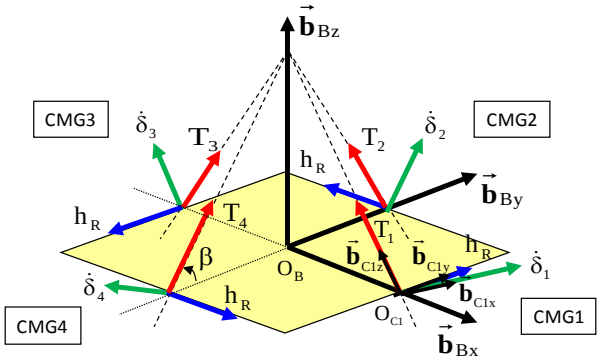

Figure 1 Definition of the coordinate

3. Attitude Control Law and Steering Law

The block diagram as shown in Fig. 2 outlines our approach. The details are explained in the following sections:

(1) Feedforward control input $\mathbf{T}_{CNT}^{ff}$ is generated as time polynomial torque profile to perform the maneuver without the flexible vibration.

(2) Feedback torque command $\mathbf{T}_{CNT}^{fb}$ is regulated in accordance with the CMG gain, which is a measure of distance from singularity, to pass singularity without the excessive gimbal rate.

(3) The combined torque command $\mathbf{T}_{CNT}$ is provided to the modified steering law. The gimbal rate command $\dot{\boldsymbol{\delta}}_{CNT}^{\alpha}$ is generated to reduce the attitude error due to misalignment.

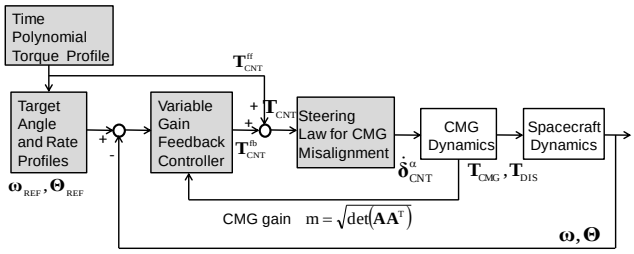

Figure 2 Block diagram of the control and steering laws

3.1. Time Polynomial Feedforward Control Law

The Nil-Mode-Exciting (NME) profiler[7] is a feedforward control input to generate the torque profile without exciting the vibration modes. It uses a sampling function with low-pass filter characteristics, and the frequency of sampling function is designed to be lower than that of 1st mode vibration. Accordingly, the multiple modes of vibration is insensitive to the input profile, and causes no residual vibration.

As for our feedforward control law, the torque profile is easily generated by using a time polynomial rather than NME profiler. To complete the rest-to-rest maneuver by the shortest angular path, the profile is formulated by using the Eigen-angle Φ about Euler's Eigen-axis $\mathbf{e}$. The time derivative of the torque (jerk) is taken into account for the boundary conditions at the initial and target orientations. This implies that the boundary conditions, including jerks, are effective to generate a smooth motion of attitude, and will suppress the modes of vibration. If a seventh power polynomial is chosen for the interpolation of the Eigen-angle profile, then the eight boundary conditions for $\Phi, \dot{\Phi}, \ddot{\Phi}$, and $\dddot{\Phi}$ at two orientations can be specified. Therefore, the torque profile $\mathbf{T}_{CNT}^{ff}$ about the Eigen-axis $\mathbf{e}$ is expressed as:

$$\begin{aligned}\mathbf{T}_{CNT}^{ff} &= I_e\ddot{\Phi}\cdot\mathbf{e} \\ &= I_e\left(12p_4t^2 + 20p_5t^3 + 30p_6t^4 + 42p_7t^5\right)\cdot\mathbf{e}\end{aligned} \tag{3.1}$$

where I_e is the moment of inertia about the Eigen-axis, and p_4, p_5, p_6, p_7 are coefficients depending on the final target Eigen-angle Φ_m and the maneuver time t_m.

In the area of hard disk drive control, the profile known as SMART (Structural Vibration Minimized Acceleration Trajectory),[11] which was formulated using jerks, had been applied to the head positioning control. It was demonstrated that SMART realizes smooth head motion, and effectively reduces the residual vibration after the head access operation.

Fig. 3 illustrates the effectiveness of the proposed torque profile. As an example, the polynomial and rectangular torque profiles, the magnitudes of which peak at 1Nm, are shown in Fig. 3(a), while their power spectrums are shown in Fig. 3(b). The spectrum of rectangular torque does not decay sufficiently in the area of high frequency, while that of polynomial torque exhibits superior roll-off characteristic. As an example, these profiles are applied to a simple spacecraft model, which has only 1st mode vibration: 0.15Hz under a free-free condition. The magnitude of the polynomial torque at 0.15Hz is

40dBNm smaller than that of rectangular torque. Figs. 3(c) and (d) show the attitude angle and rate errors with respect to the desired angle and rate profiles generated from torques shown in Fig. 3(a). In the case of the rectangular torque profile, the angle and rate errors due to 1st mode vibration are excited. After the maneuver, the spacecraft cannot start observation until the mode has been sufficiently damped. In the case of the polynomial torque profile, the attitude error is effectively suppressed at both maneuver duration (40~120sec.) and pointing duration (120sec.~).

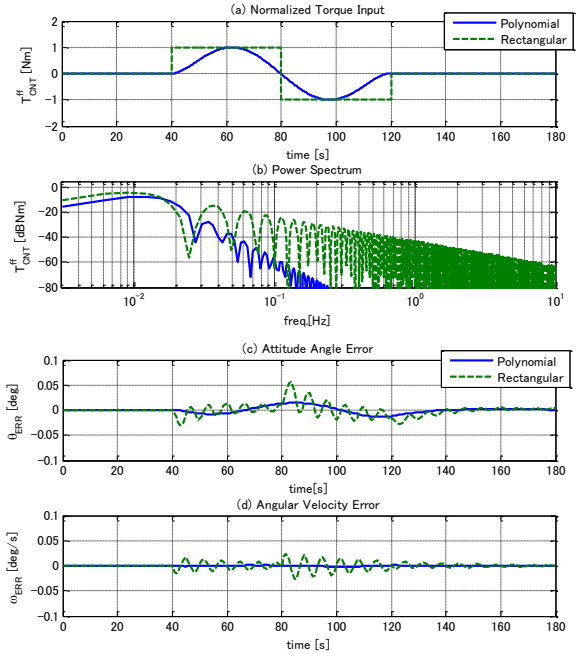

Figure 3 Characteristics of torque profiles and responses

3.2. Variable Gain Feedback Control Law

The wide bandwidth feedback controller is available for compensating for the tracking error with respect to the desired attitude profile, as described in Section 3.1. However, the feedback torque and gimbal rate command will become excessive in the vicinity of singularity for the reason explained in Section 1. If the bandwidth is designed to be narrow to avoid the above issue, the tracking accuracy far from singularity will also result in degradation.

In our approach, the magnitude of the feedback torque command is adjusted according to whether the CMGs encounter singularity or not. The torque command is expressed by using the variable attitude control gains depending on the CMG gain as follows:

$$\mathbf{T}_{\mathrm{CNT}}^{\mathrm{fb}} = \mathbf{K}_{\mathrm{d}}(\mathrm{m})\cdot\left(\boldsymbol{\omega}_{\mathrm{REF}} - \boldsymbol{\omega}\right) + \mathbf{K}_{\mathrm{p}}(\mathrm{m})\cdot\left(\boldsymbol{\Theta}_{\mathrm{REF}} - \boldsymbol{\Theta}\right) \tag{3.2}$$

where $\boldsymbol{\omega}_{\mathrm{REF}}$ and $\boldsymbol{\Theta}_{\mathrm{REF}}$ are the desired attitude rate and angle profiles generated from Eq. (3.1) respectively, while $\mathbf{K}_{\mathrm{d}}$ and $\mathbf{K}_{\mathrm{p}}$ are the derivative gain and proportional gain matrices respectively. The diagonal elements in these matrices are defined as a function of CMG gain.

$$\mathrm{k}_{\mathrm{d(p)}}^{\mathrm{m}} = \mathrm{k}_{\mathrm{d(p)}}\left\{1 - \kappa\cdot\exp\left(-\mu_{\mathrm{k}}\cdot\mathrm{m}^2\right)\right\} \tag{3.3}$$

Note that the variable gains $\mathrm{k}_{\mathrm{d}}^{\mathrm{m}}$ and $\mathrm{k}_{\mathrm{p}}^{\mathrm{m}}$ are continuously regulated in accordance with the square of CMG gain $\mathrm{m} = \sqrt{\det\left(\mathbf{A}\mathbf{A}^{\mathrm{T}}\right)}$ that approaches zero ($\mathrm{m}\approx 0$) when approaching singularity. μ_{k} is the decay rate of the variable gains. The constant derivative and proportional gains k_{d} and k_{p} are selected to provide wide bandwidth f_{C} and an appropriate damping ratio ζ_{C} respectively. Because the feedback torque command $\mathbf{T}_{\mathrm{CNT}}^{\mathrm{fb}}$ decreases according to the variable gains in the vicinity of singularity, the variable gain feedback control law works as a torque limiter.

Near singularity, because the torque command become parallel to the singular vector $\mathbf{s}$, which satisfies $\mathbf{A}^{\mathrm{T}}\mathbf{s} = \mathbf{0}$, the CMGs are unable to produce total torque about the maneuver axis. Thus, the tracking error about the maneuver axis near singularity is assumed to be allowed for in our current approach. Taking this into consideration, as depicted in Fig. 4, the scaling factor κ in Eq. (3.3) is selected as follows: $\kappa = 1$ is selected for the maneuver axis $\mathbf{e}$ and $\kappa = 0$ is selected for the other orthogonal two axes. For $\kappa = 1$, the feedback torque command about $\mathbf{e}$ is regulated by variable gains, and limited near singularity. Only the feedforward torque input of Eq. (3.1) is provided for the steering law to pass singularity. For $\kappa = 0$, the torque commands about orthogonal axes are generated by maximum constant gains k_{d} and k_{p}, the magnitudes of which are not limited, even when the configuration of CMGs are both near to, and far from, singularity respectively. The variable gain feedback control law always enables precise tracking control for orthogonal axes, while only allowing tracking error for the maneuver axis.

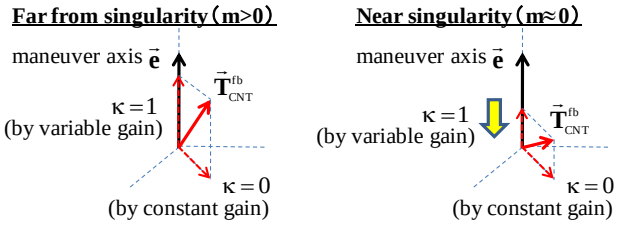

Figure 4 Torque command regulation by CMG gain m

3.3. CMG Steering Law

From the perspective of attitude control accuracy, the steering law is classified into three groups;[6] i.e. Singularity Avoidance algorithms (SA), Singularity Escape algorithms (SE), and Singularity Escape and Avoidance algorithms (SEA).

SE algorithms such as Singularity Robust inverse (SR),[1] Singular Direction Avoidance (SDA),[2] and Generalized Singularity Robust inverse (GSR),[3] intentionally add torque error to escape singularity, although the torque error adversely affects precision attitude control. Conversely, SA algorithms such as the Gradient Method (GM)[4,5] do not induce torque error, because they use an exact solution, including null-motion to avoid singularity. Therefore, SA algorithms are typically more precise than SE. However, SA algorithms cannot avoid elliptic singularities (both saturation and internal) through null-motion, while SE algorithms can escape both elliptic and hyperbolic singularities at the expense of torque error.

This paper basically adopts GSR, because it is the most robust method in the SE algorithms while allowing torque error to guarantee singularity escape. Moreover, it is based on only a pseudo-inverse solution without the null-motion, and

can thus be implemented with a simple algorithm and a low computational burden. In SE algorithms, the gimbal rate command $\dot{\boldsymbol{\delta}}_{CNT}$ is generally given with some variations of the weighting matrix $\mathbf{V}$.

$$\dot{\boldsymbol{\delta}}_{CNT} = \frac{1}{h_R}\mathbf{A}^T\left(\mathbf{A}\mathbf{A}^T + \mathbf{V}\right)^{-1}\cdot\mathbf{u} \tag{3.4}$$

$$\mathbf{u} \equiv \dot{\mathbf{H}} = -\mathbf{T}_{CNT} - \tilde{\boldsymbol{\omega}}\mathbf{H} \tag{3.5}$$

The torque error occurs due to the increase in the weighting matrix $\mathbf{V}$ near singularity.

Recently, as one of the SEA algorithms, Leve and Fitz-Coy proposed Hybrid Steering Logic (HSL) to improve tracking accuracy.[6] They combined GM to avoid hyperbolic singularity and SDA to escape elliptic singularity. HSL is successful in reducing torque error by using null-motion near hyperbolic singularity when compared with the case of SDA alone. Using a method based on the SEA algorithm may be one of the effective solutions for our approach to improve tracking accuracy near hyperbolic singularity.

4. CMG Disturbances and the Modified Steering Law

In this section, CMG disturbances induced by misalignment, gimbal friction, and rotor mass imbalances are modeled. In particular, based on the modeling of misalignment, the existing steering law described in Section 3.3 is modified.

4.1. Modeling of the CMG Misalignment Disturbance

CMG misalignment comes from the following two causes: (1) misalignment between the rotor angular momentum and gimbal axes, (2) misalignment between the gimbal axis and the spacecraft interface. Although these are minimized in the manufacturing process, a certain amount of misalignment remains in the actual CMG, which may cause undesirable angular momentum and output torque errors. In this paper, only cause (1) is considered to simplify the modeling. As shown in Fig. 5, it is assumed that an ideal rotor angular momentum vector $\vec{\mathbf{h}}_R$ is aligned about a misalignment vector $\vec{\boldsymbol{\alpha}}_i$. Accordingly, the actual rotor angular momentum vector $\vec{\mathbf{h}}_{Ri}^{\alpha}$ is written with respect to the gimbal-fixed coordinate $\{\vec{\mathbf{b}}_{Ci}\}$ for the i-th CMG.

$$\vec{\mathbf{h}}_{Ri}^{\alpha} = \vec{\mathbf{h}}_R + \vec{\boldsymbol{\alpha}}_i \times \vec{\mathbf{h}}_R = \left\{\vec{\mathbf{b}}_{Ci}\right\}^T\mathbf{h}_R + \left\{\vec{\mathbf{b}}_{Ci}\right\}^T\Delta\mathbf{h}_{Ri}^{\alpha}\left(\alpha_{ix},\alpha_{iz}\right) \tag{4.1}$$

The first term represents the ideal rotor angular momentum, and the second is the angular momentum error, including the amount of misalignment α_{ix},α_{iz}. Similarly, the actual output torque is derived using Eq. (4.1).

$$\vec{\boldsymbol{\tau}}_i^{\alpha} = \dot{\vec{\boldsymbol{\delta}}}\times\vec{\mathbf{h}}_{Ri}^{\alpha} = \left\{\vec{\mathbf{b}}_{Ci}\right\}^T\boldsymbol{\tau}_i + \left\{\vec{\mathbf{b}}_{Ci}\right\}^T\Delta\boldsymbol{\tau}_i^{\alpha}\left(\alpha_{ix}\right) \tag{4.2}$$

Eq. (4.1) is transformed to the coordinate $\{\vec{\mathbf{b}}_B\}$ using the first term of Eq. (2.3), and yields the total angular momentum error induced by 4 CMGs.

$$\Delta\mathbf{H}^{\alpha} = \sum_{i=1}^{4}\mathbf{C}_{C_i}^{B}\left(\beta,\delta_i\right)\cdot\Delta\mathbf{h}_{Ri}^{\alpha}\left(\alpha_{ix},\alpha_{iz}\right) \tag{4.3}$$

As well as Eq. (2.4), the total torque error induced by 4 CMGs is derived by differentiating Eq. (4.3) with respect to time.

$$\Delta\dot{\mathbf{H}}^{\alpha} = h_R\begin{bmatrix} \alpha_{1x}c\beta s\delta_1 & \alpha_{2x}c\delta_2 & -\alpha_{3x}c\beta s\delta_3 & -\alpha_{4x}c\delta_4 \\ -\alpha_{1x}c\delta_1 & \alpha_{2x}c\beta s\delta_2 & \alpha_{3x}c\delta_3 & -\alpha_{4x}c\beta s\delta_4 \\ -\alpha_{1x}s\beta s\delta_1 & -\alpha_{2x}s\beta s\delta_2 & -\alpha_{3x}s\beta s\delta_3 & -\alpha_{4x}s\beta s\delta_4 \end{bmatrix}\begin{bmatrix}\dot{\delta}_1\\ \dot{\delta}_2\\ \dot{\delta}_3\\ \dot{\delta}_4\end{bmatrix}$$

$$\equiv h_R\mathbf{A}^{\alpha}\left(\alpha_{ix},\beta,\delta_i\right)\cdot\dot{\boldsymbol{\delta}} \quad (i=1\sim4) \tag{4.4}$$

The introduced Jacobian $\mathbf{A}^{\alpha}$, which includes the misalignment α_{ix}, is called as Modified Jacobian in this paper. Whenever $\dot{\mathbf{H}}$ and $\mathbf{H}$ defined in Eq. (2.2) are produced for attitude control, $\Delta\dot{\mathbf{H}}^{\alpha}$ and $\Delta\mathbf{H}^{\alpha}$ are also induced. Incorporating these errors with Eq. (2.2), the actual attitude control torque is then written as

$$\mathbf{T}_{CMG}^{\alpha} = -\left\{\left(\dot{\mathbf{H}} + \Delta\dot{\mathbf{H}}^{\alpha}\right) + \tilde{\boldsymbol{\omega}}\left(\mathbf{H} + \Delta\mathbf{H}^{\alpha}\right)\right\} \equiv \mathbf{T}_{CMG} + \mathbf{T}_{DIS}^{\alpha} \tag{4.5}$$

The first term $\mathbf{T}_{CMG} = -(\dot{\mathbf{H}} + \tilde{\boldsymbol{\omega}}\mathbf{H})$ denotes the ideal attitude control torque, like Eq. (2.2), and the second term $\mathbf{T}_{DIS}^{\alpha} = -(\Delta\dot{\mathbf{H}}^{\alpha} + \tilde{\boldsymbol{\omega}}\Delta\mathbf{H}^{\alpha})$ denotes the total torque error, which acts as disturbance torque on spacecraft.

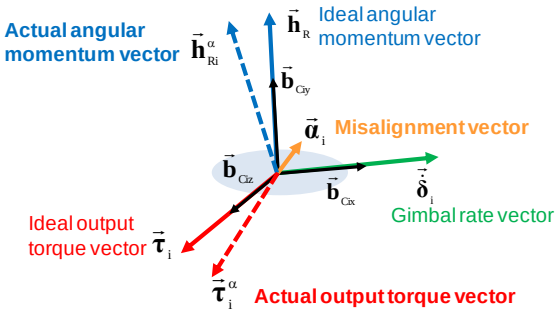

Figure 5 Modeling of the CMG misalignment

4.2. Modified Steering Law for Misalignment

It is assumed that the misalignment $\boldsymbol{\alpha}_i$ can be estimated by an on-ground measurement test in advance. Eqs. (2.4) and (4.4) are substituted into Eq. (4.5), and rewritten by

$$\mathbf{T}_{CMG}^{\alpha} = -\left\{h_R\left(\mathbf{A} + \mathbf{A}^{\alpha}\right)\cdot\dot{\boldsymbol{\delta}} + \tilde{\boldsymbol{\omega}}\left(\mathbf{H} + \Delta\mathbf{H}^{\alpha}\right)\right\} \tag{4.6}$$

As well as Eq. (3.5), the first term of Eq. (4.6) is defined by

$$\mathbf{u}^{\alpha} \equiv h_R\left(\mathbf{A} + \mathbf{A}^{\alpha}\right)\cdot\dot{\boldsymbol{\delta}} = -\mathbf{T}_{CNT} - \tilde{\boldsymbol{\omega}}\left(\mathbf{H} + \Delta\mathbf{H}^{\alpha}\right) \tag{4.7}$$

Substituting Eq. (4.7) into Eq. (4.6), $\mathbf{T}_{CMG}^{\alpha} = \mathbf{T}_{CNT}$ is obtained. This indicates that if gimbals are steered based on the torque command $\mathbf{u}^{\alpha}$, the ideal torque equal to torque command $\mathbf{T}_{CNT}$ can be produced on spacecraft. Such a gimbal rate command is obtained by a pseudo-inverse solution of Eq. (4.7), including the weighting matrix $\mathbf{V}$.

$$\dot{\boldsymbol{\delta}}_{CNT}^{\alpha} = \frac{1}{h_R}\left(\mathbf{A} + \mathbf{A}^{\alpha}\right)^T\left\{\left(\mathbf{A} + \mathbf{A}^{\alpha}\right)\left(\mathbf{A} + \mathbf{A}^{\alpha}\right)^T + \mathbf{V}\right\}^{-1}\cdot\mathbf{u}^{\alpha} \tag{4.8}$$

Eq. (4.8) is a general form of the modified steering law based on the SE algorithm, including Modified Jacobian $\mathbf{A}^{\alpha}$. Instead of Eqs. (3.4) and (3.5), the proposed Eqs. (4.7) and (4.8) are a modified steering law to reduce the attitude error in the presence of misalignment disturbance.

4.3. Modeling of Other CMG Disturbances

Various friction models have been investigated in literature. In this paper, the Karnopp model[12] is applied as a gimbal friction model, because it is a simple model to represent the stick-slip behavior. Friction torque about the gimbal axis is defined for i-th CMG as follows:

$$T_{Cix}^{F} = \begin{cases} T_{GCi} & : \left|\dot{\delta}_i\right| \le \dot{\delta}_{\varepsilon i} \quad \text{and} \quad \left|T_{GCi}\right| \le T_{SFi} \\ T_{SFi}\cdot\text{sign}\left(T_{GCi}\right) & : \left|\dot{\delta}_i\right| \le \dot{\delta}_{\varepsilon i} \quad \text{and} \quad \left|T_{GCi}\right| > T_{SFi} \\ T_{DFi}\left(\dot{\delta}_i\right) & : \left|\dot{\delta}_i\right| > \dot{\delta}_{\varepsilon i} \end{cases} \tag{4.9}$$

where T_{GCi} is gimbal motor control torque, T_{SFi} is static friction torque and T_{DFi} is dynamic friction torque. $\dot{\delta}_{\varepsilon i}$ is a small gimbal rate to represent a dead-zone. Inside the dead-zone ($|\dot{\delta}_i| \le \dot{\delta}_{\varepsilon i}$), the gimbal is supposed to be sticking. When the gimbal rate exceeds the dead-zone ($|\dot{\delta}_i| > \dot{\delta}_{\varepsilon i}$), the gimbal is supposed to be slipping. Eq. (4.9) is incorporated with the gimbal rate control-loop (PI control) in each CMG model. During the pointing, repeat of the stick-slip behavior with a small gimbal rate may result in a limit cycle around a target pointing angle.[9,10] Generally, it is known that a high gain gimbal rate feedback controller is one of the effective ways for friction compensation.

Next, the disturbance force induced by static imbalance U_{Si} and the disturbance torque induced by dynamic imbalance U_{Di} are respectively considered with respect to the coordinate $\{\vec{\mathbf{b}}_{Ci}\}$. As expressed in Eq. (2.3), the direction of the total imbalance torque $\mathbf{T}_{DIS}^{U}$ induced on the spacecraft is changed by gimballing of the rotor. Because the frequency of imbalance disturbance is synchronized to the rotor angular velocity, it is beyond the control bandwidth of ACS.

5. Numerical Simulations

Two kinds of simulations were performed to verify the performances of the proposed variable feedback gain control law and the modified steering law against the conventional laws.

5.1. Simulation for the Variable Gain Feedback Control

Consider one rigid body spacecraft maneuvering by the feedforward torque input generated by Eq. (3.1). The parameters are selected as follows: moment of inertia $\mathbf{I}$ =diag[1000,1000,1000]kgm^2, maneuver axis $\mathbf{e}$ =[0,0,1]^T (yaw axis), final target angle Φ_m =95deg, and maneuver time t_m =50sec., rotor angular momentum h_R =18Nms, skew angle β =60deg, and decay rate μ_k =10. During the maneuver, the CMGs encounter elliptic (saturation) singular configuration [90,90,90,90]deg. from the initial configuration [0,0,0,0]deg.

Fig. 6 shows the result in the case of the conventional constant gain feedback control (constant PD), with a wide bandwidth f_C =0.5Hz and damping ratio $\zeta_C = 1/\sqrt{2}$ for 3 axes. Fig. 7 shows the result in the case of the proposed variable feedback gain control (variable PD), which has the variable gains for the yaw axis and the constant gains for another two axes. As can be seen in Fig. 6, during the singularity $m \approx 0$ (30~46sec.), the excessive feedback torque command about yaw axis is caused, although the gimbals cannot respond to the demanded torque command. The gimbal rate becomes immediately so large, at about 5rad/s at the end of singularity (46sec.), due to the excessive torque command. Such a large gimbal rate is difficult to generate in practice, and results in degradation of attitude accuracy. As shown in Fig. 7, during the singularity $m \approx 0$ (30~38sec.), the variable gains become almost zero in order to limit the torque command about the yaw axis. Right after passing singularity (38sec.~), the torque command is slowly increased according to the increase in gains, and the resulting gimbal rate is mitigated within a small value not exceeding 1rad/s. Therefore, the proposed variable feedback control law enables the spacecraft to pass singularity within an acceptable gimbal rate and continue the precise tracking control.

5.2. Simulation for the Modified CMG Steering Law

As shown in Table 1, CMG disturbances are included in the simulation. It is assumed that the magnitude of torque error $\Delta\boldsymbol{\tau}_i^{\alpha}$ due to misalignment is 1~4% compared with the magnitude of ideal output torque $\boldsymbol{\tau}_i$. The feedforward torque input is generated as well as Section 5.1: $\mathbf{e}$ =[0,0,1]^T, Φ_m =60deg, and t_m =50sec. The spacecraft completes the maneuver without encountering singularity, so that the feedback gains are maintained almost constant.

Fig. 8 shows the result in the case of the conventional GSR[3], as represented by Eqs. (3.4) and (3.5). Fig. 9 shows the result in the case of the modified GSR represented by Eqs. (4.7) and (4.8). As can be seen in Fig. 8, the attitude angle and rate errors due to misalignment appear during the gimbal steering (10~60sec.). Conversely, as shown in Fig. 9, both angle and rate errors are reduced almost to zero.

During the pointing (60sec.~) in Fig. 8, the spacecraft attitude falls into the limit cycle due to gimbal friction, due to the narrow bandwidth of the gimbal rate control-loop at 10Hz. Conversely, the attitude errors are reduced because the wide bandwidth controller 20Hz is applied in Fig. 9. The attitude errors in both Figs. 8 and 9 include the jitter due to imbalance disturbances.

Table 1 Disturbance parameters for i-th CMG

Parameter		Value
Misalignment $\boldsymbol{\alpha}_i = [\alpha_{ix} \quad \alpha_{iy} \quad \alpha_{iz}]^T$ $\boldsymbol{\alpha}_1$ =[0.01, 0, 0.01]^T, $\boldsymbol{\alpha}_2$ =[0.02, 0, 0.02]^T $\boldsymbol{\alpha}_3$ =[0.03, 0, 0.03]^T, $\boldsymbol{\alpha}_4$ =[0.04, 0, 0.04]^T		
Static imbalance Dynamic imbalance	U_{Si} U_{Di}	0.1gcm 1.0gcm^2
Static friction torque	T_{SFi}	0.07Nm
Dynamic friction torque (only coulomb friction)	T_{DFi}	0.05Nm
Dead-zone gimbal rate	$\dot{\delta}_{\varepsilon i}$	0.0001rad/s

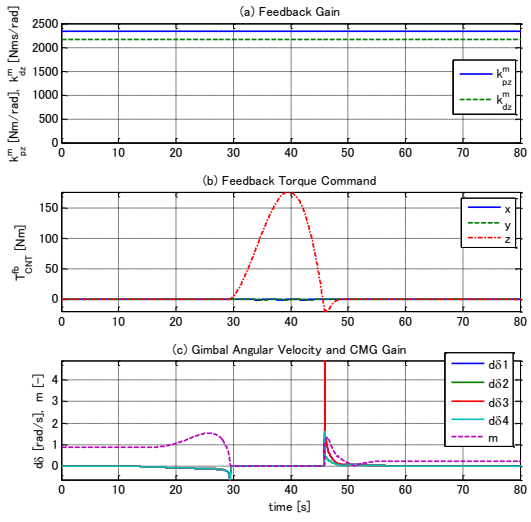

Figure 6 Conventional constant gain feedback control

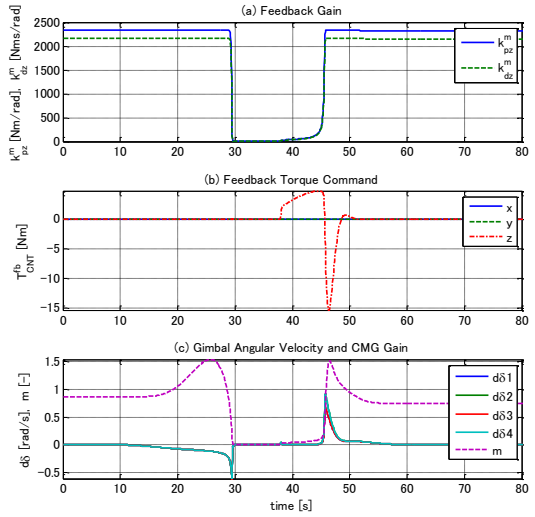

Figure 7 Proposed variable gain feedback control

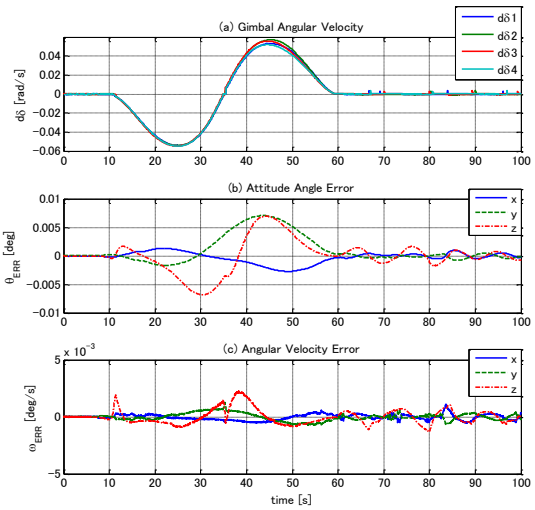

Figure 8 Conventional GSR steering law

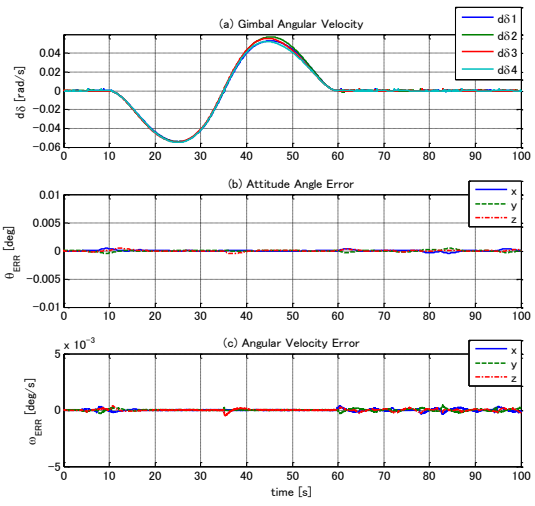

Figure 9 Modified GSR steering law

6. Conclusion

This paper presented the feedforward/feedback control laws and steering law to improve tracking and pointing accuracies during the agile maneuvers. The following results were shown: (1) The time polynomial feedforward control law effectively suppresses attitude error induced by vibration due to flexible appendages, (2) The variable gain feedback control law is a simple yet effective way to mitigate the excessive gimbal rate in the vicinity of singularity, and allows spacecraft to continue precision tracking control, (3) The modified steering law is effective in reducing the attitude error induced by CMG misalignment.

In relation to (2), the torque error near singularity is currently allowed in our approach. The SEA algorithm may be one of the effective ways to improve tracking accuracy near hyperbolic singularity.

References

1) Bedrossian, N. S., Paradiso, J., Bergmann, E. V., and Rowell, D., “Steering Law Design for Redundant Single-Gimbal Control Moment Gyroscopes”, *J. Guidance, Control, and Dynamics*, Vol. 13, No. 6, 1990, pp. 1083-1089.
2) Ford, K. A., and Hall, C. D., “Singular Direction Avoidance Steering for Control-Moment Gyros”, *J. Guidance, Control, and Dynamics*, Vol. 23, No. 4, 2000, pp. 648-656.
3) Wie, B., Bailey, D., and Heiberg, C., “Singularity Robust Steering Logic for Redundant Single-Gimbal Control Moment Gyros”, *J. Guidance, Control, and Dynamics*, Vol. 24, No. 5, 2001, pp. 865-872.
4) Yoshikawa, T., ”A Steering Law for Three Double Gimbal Control Moment Gyro System”, NASA TM X-64926.
5) Cornick, D. E., “Singularity Avoidance Control Laws for Single Gimbal Control Moment Gyros”, AIAA paper 79-1698, 1979, pp. 20-33.
6) Leve, F. A., and Fitz-Coy, N. G., “Hybrid Steering Logic for Single-Gimbal Control Moment Gyroscopes”, *J. Guidance, Control, and Dynamics*, Vol. 33, No. 4, 2010, pp. 1202-1212.
7) Kamiya, T., Ogura, N., Maeda, K., and Sakai, S., “Preshaping Profiler for Astro-G Rest-to-Rest Maneuvers”, *J. Space Technology and Science*, Vol. 25, No. 1, 2009, pp. 41-47.
8) Singhose, W., Derenzinski, S., and Singer, N., ”Extra-Insensitive Input Shapers for Controlling Flexible Spacecraft”, *J. Guidance, Control, and Dynamics*, Vol. 19, No. 2, 1996, pp. 385-391.
9) Liden, S. P., “Precision CMG Control for High-Accuracy Pointing”, *J. Spacecraft and Rockets*, Vol. 11, No. 4, 1974, pp. 236-240.
10) Seltzer, S.M., “CMG-Induced LST Dynamics”, NASA TM X-64833, 1974.
11) Mizoshita, Y., Hasegawa, S., and Takaishi, K., “Vibration Minimized Access Control For Disk Drives”, *IEEE. Trans. Magnetics*, Vol. 32, No. 3, 1996, pp. 1793-1798.
12) Karnopp, D., “Computer Simulation of Stick-Slip Friction in Mechanical Dynamic Systems”, *J. Dynamic Systems, Measurement, and Control*, Vol. 107, 1985, pp. 100-103.